Journal Pre-proofs

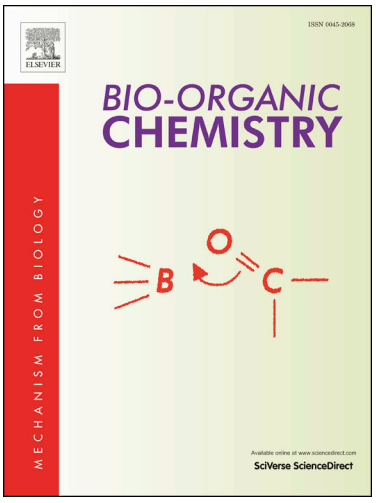

Development of small-molecule BRD4 degraders based on pyrrolopyridone derivative

Jian Zhang, Pan Chen, Peiyu Zhu, Peiyuan Zheng, Tao Wang, Lixun Wang, Changliang Xu

PII: S0045-2068(19)32264-3
DOI: https://doi.org/10.1016/j.bioorg.2020.103817
Reference: YBIOO 103817

To appear in: *Bioorganic Chemistry*

Received Date: 31 December 2019
Revised Date: 31 March 2020
Accepted Date: 2 April 2020

Please cite this article as: J. Zhang, P. Chen, P. Zhu, P. Zheng, T. Wang, L. Wang, C. Xu, Development of small-molecule BRD4 degraders based on pyrrolopyridone derivative, *Bioorganic Chemistry* (2020), doi: https://doi.org/10.1016/j.bioorg.2020.103817

Development of small-molecule BRD4 degraders based on pyrrolopyridone derivative

Jian Zhang[a], Pan Chen[b], Peiyu Zhu[a], Peiyuan Zheng[a], Tao Wang[a], Lixun Wang[a], Changliang Xu[c,*], ord[a] *Center of Drug Discovery, Jiangsu Key Laboratory of Drug Discovery for Metabolic Disease, China Pharmaceutical University, Nanjing 210009, PR China*

[b] *Department of Medicinal Chemistry, China Pharmaceutical University, Nanjing 210009, PR China*

[c] *Jiangsu Collaborative Innovation Center of Traditional Chinese Medicine Prevention and Treatment of Tumor, Nanjing University of Chinese Medicine, Nanjing 210023, PR China*

Abstract

Bromodomain-containing protein 4 (BRD4) plays a crucial role in the epigenetic regulation of gene transcription and some BRD4 inhibitors have been advanced to clinical trials. Nevertheless, the clinical application of BRD4 inhibitors could be limited by drug resistance. As an alternative strategy, the emerging Proteolysis Targeting Chimeras (PROTACs) technology has the potential to overcome the drug resistance of traditional small-molecule drugs. Based on PROTACs approaches, several BRD4 degraders were developed and have been proved to degrade BRD4 protein and inhibit tumor growth. Herein, we present the design, synthesis, and biological evaluation of pyrrolopyridone derivative-based BRD4 degraders. Four synthesized compounds displayed comparative potence against BRD4 BD1 with IC_{50} at low nanomolar concentrations. Anti-proliferative activity of **32a** against BxPC3 cell line (IC_{50} = 0.165 μM) was improved by about 7-fold as compared to the BRD4 inhibitor ABBV-075. Furthermore, degrader **32a** potently induced the degradation of BRD4 and inhibited the expression of c-Myc in BxPC3 cell line in a time-dependent manner. The exploration of intracellular antitumor mechanism showed **32a** induced cell cycle arrest and apoptosis effectively. All the results demonstrated that compound **32a** could be considered as a potential BRD4 degrader for further investigation.

1. Introduction

Lysine acetylation of histones is a momentous post-translational modification of gene transcription [1,2]. By recognizing the acetylated lysine (KAc) residues on histone tails, bromodomain-containing proteins (BCPs) participate in the epigenetic regulation of the gene expression as epigenetic "readers" and they are related to various diseases such as cancer, neurological disorders, inflammation and metabolic disorders [2-4]. Among these BCPs, the bromodomain and extra-terminal domain (BET) family proteins (BRD2, BRD3, BRD4, and BRDT) have gained much importance in recent years for their essential physiological functions [5-8]. Bromodomain-containing protein 4 (BRD4) is the most extensively studied protein of BET family and plays an essential role in different signaling pathways. BRD4 promotes transcriptional elongation by recruiting of the positive transcription elongation factor b (P-TEFb) for stimulating phosphorylation of RNA polymerase II [5,9,10]. The c-Myc protein is abnormally expressed in most malignant tumors as a pivotal factor in regulating cell proliferation, and blocking the binding of BRD4 and acetyl histone can significantly down-regulate the transcription of c-Myc gene [11-13]. Prior research generally confirms that BRD4 is an ideal target for a great many of cancers such as leukemia, lymphoma, nuclear protein in testis (NUT) midline carcinoma, prostate cancer, and pancreatic cancer [12-16].

With the identification of first potent BRD4 inhibitor **1** ((+)-JQ-1) (**Fig. 1**) [14], a great number

of researches have been devoted to the development of BRD4 inhibitors and numerous candidates with different scaffolds including **2** (I-BET762), **3** (OTX-015), **4** (CPI-0610), and **5** (ABBV-075), have been put into clinical research for the treatment of human cancers (**Fig. 1**) [17-20]. In addition to single administration, combination strategy of BRD4 inhibitors with other antineoplastic drugs such as histone deacetylase inhibitor or BCL2 inhibitor brings significant improvement to the efficacy of chemotherapy [16,21]. Single or combined administration of BRD4 inhibitors has significant effects in the treatment of many kinds of tumors, and BRD4 has become a promising target for the development of cancer therapeutic drugs. While preclinical and clinical studies have demonstrated the enormous therapeutic potential of BRD4 inhibitors, the tumour resistance to BRD4 inhibitor was found in certain contexts, for example, BRD4 promotes transcription and cell proliferation in BET-resistant TNBC cells in a bromodomain-independent mode [22,23]. Furthermore, BRD4 inhibitors lead to significant BRD4 protein accumulation and inefficient c-Myc suppression [24]. Thus, alternative therapeutic modalities are needed which can address these problems.

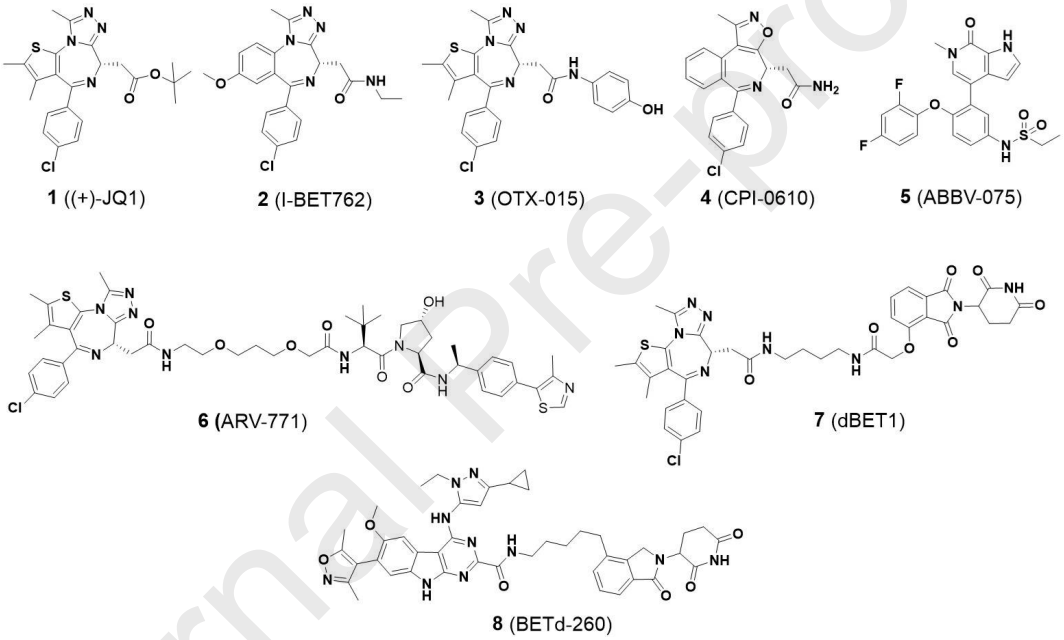

Fig. 1. Chemical structures of representative BRD4 inhibitors (**1-5**) and BRD4 degraders (**6-8**)

A novel method to induce the degradation of pathogenesis-related proteins using the Proteolysis Targeting Chimeras (PROTACs) has attracted broad attention as a promising strategy in drug discovery [24-28]. PROTACs (also known as degraders) are reasonably designed bifunctional molecules that consist of a ligand of the protein of interest (POI), a ligand capable of recruiting E3 ubiquitin ligase, and an applicable linker that connects two ligands. By simultaneously binding of POI and E3 ubiquitin ligase, the heterobifunctional molecule induces the formation of a ternary complex, followed by ubiquitination and proteasome-dependent degradation of the target protein [24,29]. Owing to the irreversible degradation instead of inhibition, PROTACs have exhibited comparative advantages over small-molecule inhibitors including targeting the undruggable proteins, overcoming drug resistance, increasing *in vitro/in vivo* potency, and improving pharmacodynamic effect *in vivo* [30,31]. The rapid development of targeted protein degradation benefit from the identification of several small-molecule ligands of E3 ubiquitin ligase especially cereblon (CRBN)，a component of the E3 ubiquitin ligase complex $CRL4^{CRBN}$, was

identified as the target protein of thalidomide and its analogues (**9**, pomalidomide and **10**, lenalidomide) (**Fig. 2**) which have been approved by the FDA as immunomodulatory drug (IMiDs) [32,33]. Recently, a number of BRD4 degraders were proved to be powerful in the degradation of BRD4 protein and degradation-based antitumor activity including **6** (ARV-771) [34], **7** (dBET1) [25], and **8** (BETd-260) (**Fig. 1**) [35]. ARV-771, a BRD4 degrader derived from (+)-JQ-1, showed significant anti-proliferation and pro-apoptosis effects on castration-resistant prostate cancer (CRPC) cells, resulted in rapid BRD4 protein degradation with DC_{50} values < 1 nM, and had an excellent potency on the treatment of CRPC [34]. BETd-246 and its analogue BETd-260 potently degraded BRD4 protein and showed strong antitumor effects *in vivo* against triple-negative breast cancers, which are lack of recognized therapeutic targets [36].

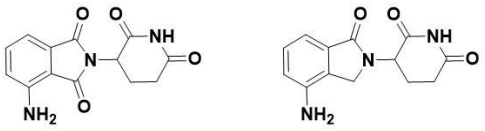

9 (pomalidomide) **10 (lenalidomide)**

Fig. 2. Chemical structures of pomalidomide and lenalidomide

PROTAC BRD4 degraders exhibited increased anti-tumor activities *in vitro/in vivo* and favorable pharmacokinetic properties. New BRD4 degraders with different scaffolds are worthy to explore their therapeutic potential in different cancers. Herein, we would like to describe our work on the design, synthesis and biological evaluation of BRD4 degraders based on pyrrolopyridone derivative. All the synthesized compounds were evaluated for their binding affinities against BRD4 BD1 and anti-proliferative effects on several tumor cell lines. Then the degradation of BRD4 and influence on the expression of c-Myc that induced by degraders **32a** and **32b** was performed on BxPC3 cell line using Western blot analysis. Moreover, analyses of cell cycle progression and apoptosis also were carried out to elucidate the intracellular mechanism of cell viability caused by the depletion of BRD4. The preferred degrader **32a** with excellent BRD4 inhibition activity and anti-proliferative activity was found to be the most effective and worthy of further investigation.

2. Results and discussion

2.1 Design strategy

The clinical candidate **5** (ABBV-075), which have been effectively applied to the therapy of various cancers (e.g. castration-resistant prostate cancer, triple negative breast cancer, small-cell lung cancer, and acute myeloid leukemia) [21,37-39], was selected as the BRD4 binding moiety to construct our desired BRD4 degraders. To understand the binding mode between BRD4 with ABBV-075, we performed docking studies with Glide docking. The X-ray cocrystal structure of pyrrolopyridone derivative A-1359643 in complex with BRD4-BD2 (PDB ID: 5UVX) revealed the important interactions of the pyrrolopyridone core with the conserved Asn433. The pyridone carbonyl formed a hydrogen bond to the NH_2 of Asn433, and the pyrrole NH accepted a hydrogen bond from the Asn433 carbonyl (**Fig. S1A**) [38]. A-1359643 was docked into BRD4-BD1 crystal complex (PDB ID: 5EI4) and the valuable interactions of the pyrrolopyridone core with the conserved Asn140 were maintained (**Fig. S1C**). Consistent with the above results, docking of ABBV-075 to BRD4-BD2 (PDB ID: 5UVX) or BRD4-BD1 (PDB ID: 5EI4) indicated a similar binding mode for the interaction of the pyrrolopyridone core with the conserved Asn residue (**Fig. S1B and S1D**). We assumed that the pyrrole ring of ABBV-075 was a suitable modification site.

Furthermore, the previous studies on the derivation of the pyrrole ring have demonstrated that the side chain substitution of pyrrole ring is tolerable to maintain the affinity against BRD4 [40,41]. We hypothesized it is also acceptable that the linkers connected with the E3 ligase ligand were introduced in the pyrrole ring. Thus, the pyrrolopyridone derivative **25** was obtained by amide condensation of intermediate **24** with the propargylamine (**Scheme 1**), which was used to yield the structure of triazole. A PROTAC-mediated ternary complex depends on the minimum linker length so that the proteins can bind together without incurring steric conflicts, and different composition and length of each linker determine the strength of PROTAC to bind to and stabilize the ternary complex, thus affecting ubiquitination and proteasome-dependent degradation of the target protein [42]. We explored different PEG lengths considering the importance of the linker length to exert degradation activity of degraders. Since immunomodulatory drugs were utilized to effectively generate PROTACs, lenalidomide (**10**) was employed as a recruiting moiety for E3 ligase CRBN.

2.2. Chemistry

As shown in **Scheme 1**, intermediate **25** was synthesized according to the references [40,41]. Nucleophilic substitution reaction of commercially available **11** with 2,4-difluorophenol afforded compound **12**. The intermediate **14** was obtained by reduction of **12** with iron powder, followed by sulfonylation of amine **13**. The intermediate **17** was prepared by reduction of compound **16** employing iron powder, which was derived from condensation of 5-bromo-2-methoxy-4-methyl-3-nitropyridine (**15**) with diethyl oxalate. N-benzyl protection of **17** provided intermediate **18**. The compound **20** was synthesized by demethylation of **18** in the presence of 4 N HCl, followed by N-methylation with dimethyl sulfate. The pinacol arylboronate (**21**) was prepared by coupling reaction of **20** with bis- (pinacolato) diboron. Suzuki coupling reaction of **21** with intermediate **14** gave compound **22**. The ester **23** was yielded by N-deprotection of **22**. Hydrolysis of **23** delivered compound **22,** which afforded intermediate **25** by the amide condensation of compound **24** with propargylamine.

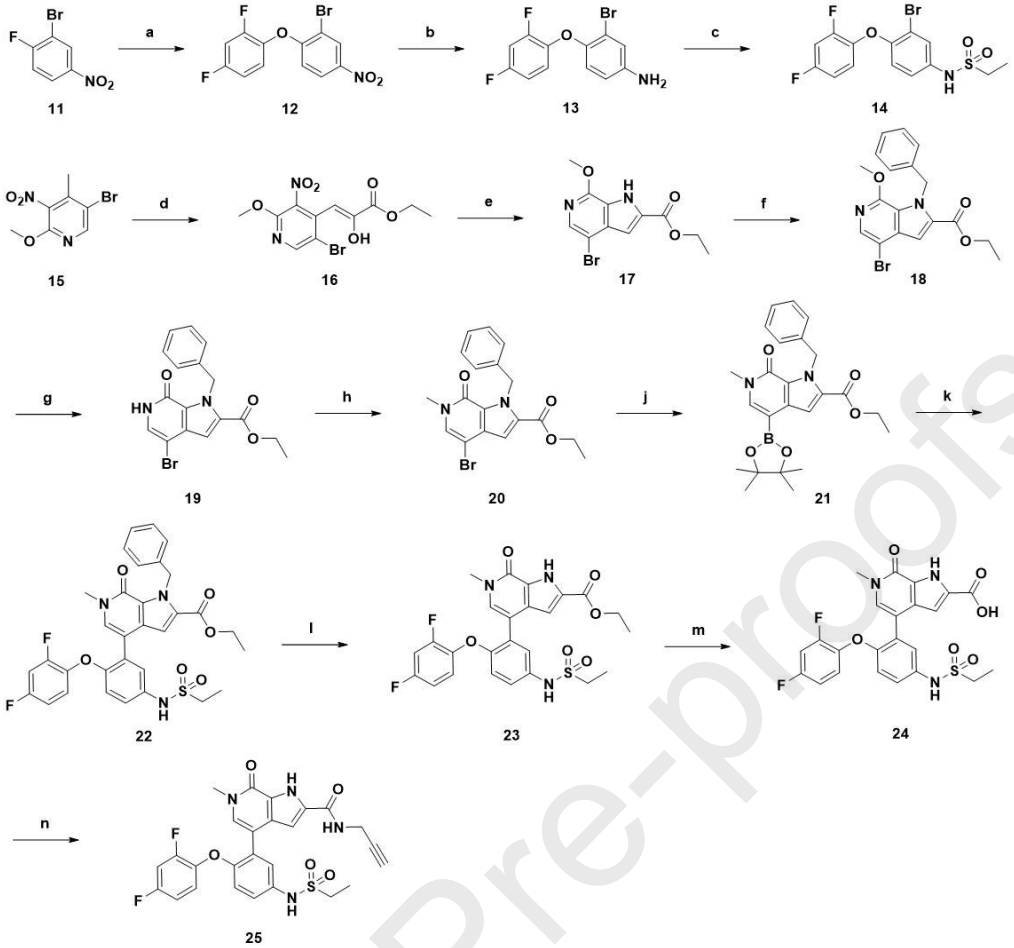

Scheme 1. The synthesis of intermediate **25**. Reagents and conditions: (a) 2,4-difluorophenol, K_2CO_3, DMF, 85°C; (b) Fe, NH_4Cl, EtOH/THF, 100°C; (c) (i) ethanesulfonyl chloride, triethylamine, DCM, 0°C to rt; (ii) 10% NaOH, 1,4-dioxane, 100°C; (d) diethyl oxalate, C_2H_5OK, C_2H_5OH/ether, 40°C; (e) Fe, C_2H_5OH/CH_3COOH, 80°C; (f) benzyl bromide, K_2CO_3, DMF, 80°C; (g) 4 N HCl, 1,4-dioxane, 80°C; (h) Me_2SO_4, K_2CO_3, acetonitrile, 70°C; (i) bis(pinacolato)diboron, tris(dibenzylideneacetone)dipalladium, X-PHOS, KOAc, 1,4-dioxane, 80°C; (j) **14**, $Pd(dppf)Cl_2 \cdot CH_2Cl_2$, K_2CO_3, toluene/MeOH/DMF, 80°C; (k) anisole, conc. H_2SO_4, CF_3COOH, 60°C; (l) $LiOH \cdot H_2O$, $MeOH/H_2O$, 60°C; (m) propargylamine, EDCI, HOBT, TEA, DMF, rt.

The synthetic procedures of target compounds **32a-32d** are outlined in **Scheme 2**. Treatment of commercially available **26a-26d** with 4-tosyl chloride delivered compounds **27a-27d**, which afforded intermediates **28a-28d** by nucleophilic substitution with sodium azide. Analogues **30a-30d** were prepared by deprotection of compounds **29a-29d** with trifluoroacetic acid, which was derived from nucleophilic substitution of tert-butyl bromoacetate with **28a-28d**. The intermediates **30a-30d** were reacted with thionyl chloride to provide chloride intermediates, which were converted to derivatives **31a-31d** by amide condensation with lenalidomide. Finally, target compounds **32a-32d** were synthesized by "Click Reaction" of **31a-31d** with intermediate **25** in the presence of copper sulfate pentahydrate and sodium ascorbate.

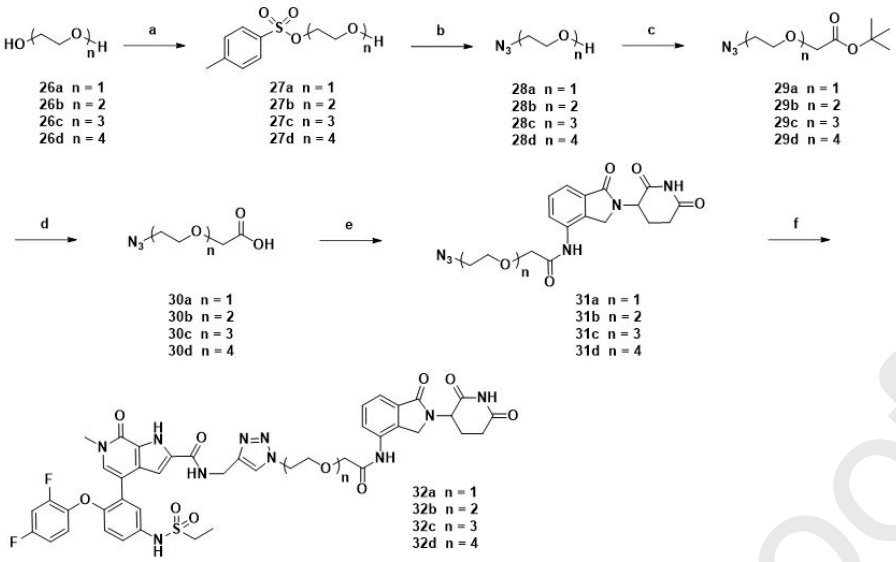

Scheme 2. The synthesis of target compounds **32a-32d**. Reagents and conditions: (a) 4-tosyl chloride, pyridine, rt; (b) sodium azide, propanone/H_2O, 60°C; (c) tert-butyl bromoacetate, sodium hydride, THF, 0°C to rt; (d) CF_3COOH, DCM, rt; (e) (i) thionyl chloride, DMF, DCM; (ii) lenalidomide, 1-methyl-2-pyrrolidinone, rt; (f) **25**, $CuSO_4 \cdot 5H_2O$, sodium ascorbate, MeOH/DCM/H_2O, rt.

2.3 In vitro BRD4 BD1 inhibitory activities

The binding affinities against BRD4 BD1 of the synthesized target compounds were evaluated by an AlphaScreen assay, and ABBV-075 was selected as the reference compound. The inhibitory activities are summarized in **Table 1**. All the degraders exhibited robust potency against BRD4 BD1 with the values of IC_{50} at low nanomole levels, which showed comparative efficiency with the positive control (ABBV-075: IC_{50} = 2.5 nM). Degrader **32a,** with the shortest PEG linker, showed the greatest efficacy for the inhibition of BRD4 BD1 (**32a**: IC_{50} = 2.7 nM). Compounds **32b** and **32c** were obtained by increasing the length of the PEG linker, and their binding affinities were also maintained (**32b**: IC_{50} = 3.4 nM; **32c**: IC_{50} = 3.7 nM). The IC_{50} of compound **32d** was decreased by more than four-fold when 4-PEG was introduced into the linker (**32d**: IC_{50} = 12.0 nM). In general, the screening of protein–ligand binding affinities demonstrated our hypothesis that the introduction of side chains to the pyrrole ring is feasible to maintain the BRD4 BD1 inhibitory activity of the synthesized degraders.

Table 1

The IC_{50} values of BRD4 BD1 for target compounds **32a-32d** and their anti-proliferation activities against BxPC3 cell line

Compound	BRD4 BD1 Alpha Screen IC_{50} (nM)[a]	IC_{50} (BxPC3, μM)[a]
32a	2.7	0.165
32b	3.4	0.245
32c	3.7	4.138
32d	12.0	> 10
ABBV-075	2.5	1.216

[a] The date presented are the mean values of at least three independent determinations.

2.4 Anti-proliferative effects against cancer cell lines in vitro

To determine the effect of degraders on the anti-proliferation activity of cancer cells, we performed MTT assay of synthesized compounds on several different solid tumor cell lines including DLD-1, HCT-116, BxPC3, MDA-MB-231, A549 and PC-9. Among them, human pancreatic cancer cell line (BxPC3) showed the best sensitivity to our PROTACs. The semi-inhibitory concentration (IC_{50}) values of degraders **32a-32d** on BxPC3 were outlined in **Table 1**. Compared to the BET inhibitor ABBV-075 (IC_{50} = 1.216 μM), the degraders **32a** and **32b** exhibited stronger anti-proliferative potency (**32a**: IC_{50} = 0.165 μM; **32b**: IC_{50} = 0.245 μM) against BxPC3 cell line. As illustrated in **Fig. S2,** the degraders **32a** and **32b** showed potent anti-proliferation activity in a concentration-dependent manner, and those compounds were subsequently selected to investigate the ability to induce BRD4 degradation. While compounds **32c** had moderately reduced inhibitory activity against BxPC3 cells, the anti-proliferative effect of **32d** dropped significantly, which underlined that the length of linker is crucial for the physiological activity of PROTACs. As showed in **Table S1**, in some tumor cell lines, the anti-proliferation effect of **32c** was even better than that of **32a** and **32b**. We speculated that the inability of **32c** to efficiently poly-ubiquitinate BRD4 protein in BXPC3 cells might underlie the reduced activity.

2.5 Degradation of BRD4 and influence on expression of c-Myc

To elucidate the degradation potency of synthesized compounds, the degradation of BRD4 induced by degraders **32a** and **32b** was identified on BxPC3 cell line using Western blot analysis. **10** (lenalidomide), **5** (ABBV-075), and their combination were used as the reference groups. Cells were treated with compounds as indicated at the concentration of 1 μM for 48 h. Compared to the control groups, **32a** and **32b** almost completely degraded BRD4 protein as shown in **Fig. 3A** and **3B**. The reference groups had no significant influence on the degradation of BRD4 except ABBV-075, which indicated a slight decrease in the level of BRD4. These results confirmed that the degradation of the target protein was induced by the designed degraders. As our compounds were proved to be efficacious in binding to BRD4, we also performed an evaluation on the expression of c-Myc, a downstream protein of BRD4-mediated signaling pathway. The expression level of c-Myc was reduced to varying degrees in the presence of PROTACs or **5**. Especially, degraders **32a** and **32b** showed superior regulatory effect on the downregulation of c-Myc. Interestingly, the expression of c-Myc was increased by more than two-fold in the group treated with **10** (lenalidomide), which could be induced by negative feedback. Because of the inhibitory effect of ABBV-075 on the expression of c-Myc, the high expression of cMyc for lenalidomide only was reduced by the combination of lenalidomide and ABBV-075.

(A)

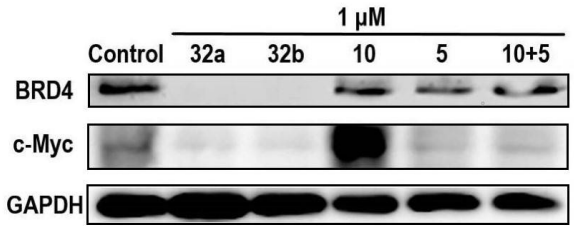

(B)

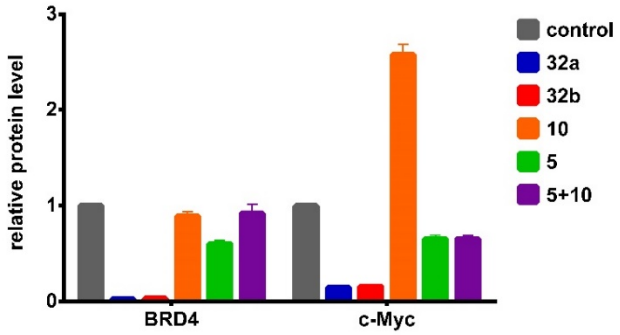

Fig. 3. (A) Western blot analysis of BRD4 and c-Myc in BxPC3 cells treated with indicated compounds at the concentration of 1 μM for 48 h; (B) Grayscale analysis of protein levels of BRD4 and c-Myc measured by Image J.

In order to gain insights into the degradation of BRD4, we characterized the degradation efficacy of the preferred compound **32a** at different indicated time points. BxPC3 cells were treated with degrader **32a** at the concentration of 1 μM for 48 h. As illustrated in **Fig. 4A** and **4B**, the significant degradation of BRD4 was detected as early as 1 h after the treatment of **32a**, followed by a maximum degradation of BRD4 while the cells were treated for 8 h. Degrader **32a** gradually inhibited the expression of c-Myc from 2 h after the administration, and had the strongest repressive effect after 48-hour treatment. The degradation of BRD4 by PROTACs sustained during the administration as well as the inhibition of c-Myc expression. Cells were washed with PBS and the new drug-free medium was added after treatment of 8 h. Interestingly, the level of BRD4 and c-Myc both had a moderate recovery, and failed to restore the initial level. The decrease of c-Myc expression at 48 h post washout might be related to the stationary phase of cell proliferation in the culture medium. In brief, the degrader **32a** time-dependently degraded BRD4 protein and inhibited the expression of c-Myc.

(A)

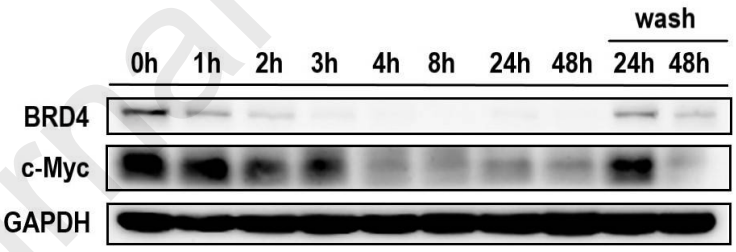

(B)

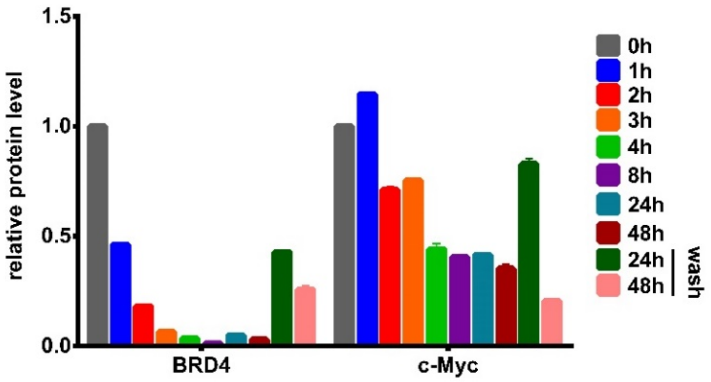

Fig. 4. (A) Western blot analysis of BRD4 and c-Myc in BxPC3 cells treated with compound **32a** (1 μM) at different

indicated time points; (B) Grayscale analysis calculated by Image J for protein levels of BRD4 and c-Myc at different indicated time points.

2.6 Analysis of cell cycle progression and apoptosis

To explore the intracellular mechanism of anti-proliferation activity generated by our designed degraders, we performed cell cycle progression and apoptosis analysis in BxPC3 cell line through flow cytometry. As mentioned above, BxPC3 cells were treated with **32a**, **32b** and other reference groups for 48 h. Except the lenalidomide-treated group, treatment with compounds resulted in cell cycle change, including an increase in G0/G1 and G2/M phase cells, and a decrease of S phase cells as shown in **Fig. 5A**. Obviously, the degrader **32a** exhibited a superior potency on G0/G1 phase cell cycle arrest. Subsequently, cell apoptosis in diverse degrees were observed in the presence of degrader and **5** (ABBV-075) as outlined in **Fig. 5B**. The PROTACs **32a** and **32b** were more potent than BRD4 inhibitor in inducing apoptosis on BxPC3 cells.

(A)

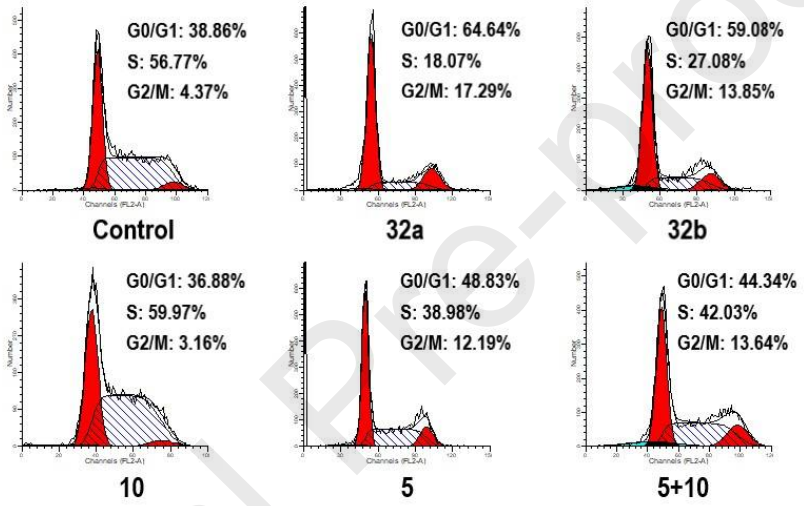

(B)

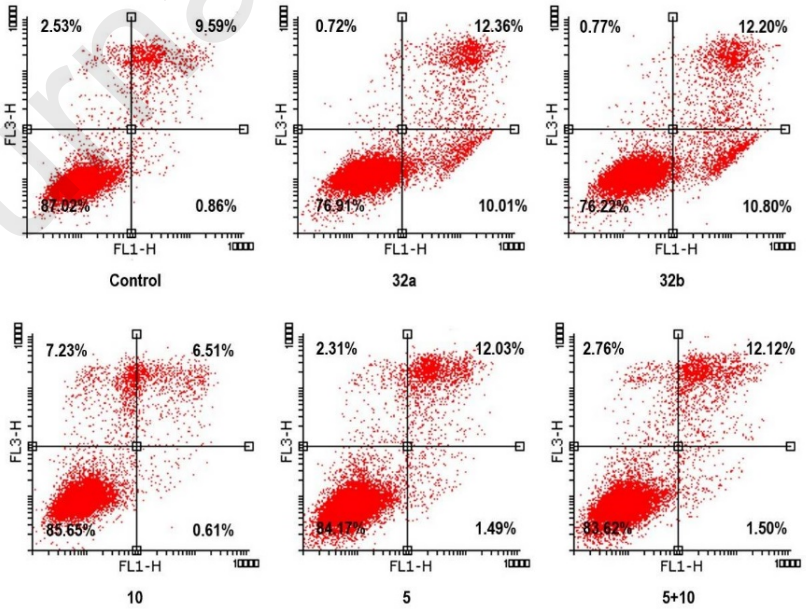

Fig. 5. Analysis of cell cycle progression (A) and apoptosis (B) in BxPC3 cells treated with all indicated compounds at the concentration of 1 μM for 48 h. The figures are representative of three separate experiments.

To further verify the effect of compounds on cell apoptosis, the live-dead staining of BxPC3 cells was carried out. As illustrated in **Fig. 6A and S3**, the degrader **32a** showed the optimal potency in inducing apoptosis, followed by a moderate apoptosis induced by **32b** and **5** (ABBV-075). We also explored the expression of apoptosis-related proteins as shown in **Fig. 6B** and **S4**. Degrader **32a** and **32b** significantly downregulated the expression of anti-apoptotic protein Bcl-xl and promoted the apoptosis of BxPC3 cells. Meanwhile, early apoptotic events were already apparent as the activation of key apoptosis protease (caspase 3 and cleaved-caspase 3) was induced by **32a** and **32b**. These results demonstrated that the synthesized degraders potently induced cell apoptosis, which might contribute to the robust anti-proliferative effects against BxPC3 cell line.

(A)

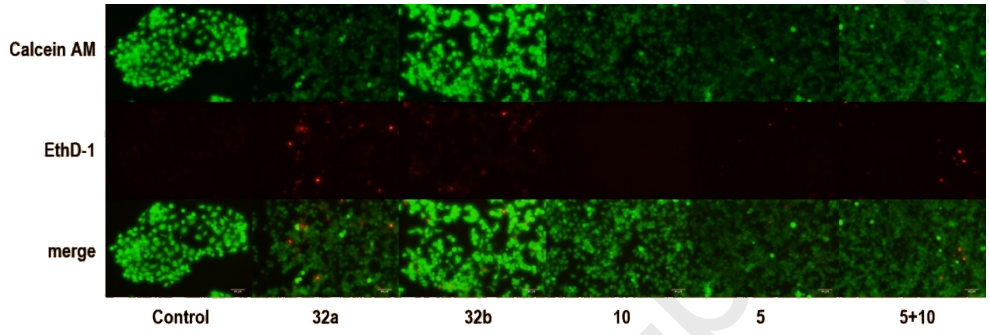

(B)

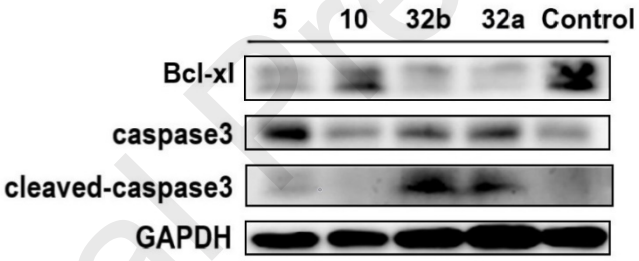

Fig. 6. (A) Live-dead cell staining of the BxPC3 cells treated with indicated compounds at the concentration of 1 μM for 48 h; (B) Western blot analysis of apoptosis-related proteins in BxPC3 cells treated with indicated compounds at the concentration of 1 μM for 48 h. The figures are representative of three separate experiments.

3. Conclusion

In summary, we designed and synthesized a series of novel small-molecule BRD4 degraders based on pyrrolopyridone derivative employing PROTACs technique, and their biological effects were evaluated. All degraders maintained potent binding affinities against BRD4 BD1. The compounds **32a** and **32b** exhibited better anti-proliferative activities on BxPC3 cell line compared to BRD4 inhibitor, and almost completely degraded BRD4 protein. The degradation of BRD4 was significantly induced by the preferred compound **32a** in a time-dependent manner, which resulted in the continuous decrease of c-Myc expression. Further mechanism study indicated that degrader **32a** could effectively induce the cell cycle arrest and apoptosis. These results highlighted the therapeutic potential of PROTACs on human pancreatic cancer. The optimization of BRD4 degraders as well as the other physiological effects will be administered in the future investigation.

4. Experimental section

4.1 Chemistry

All commercial solvents or reagents were analytically or chemically pure products and were directly used without further treatment unless otherwise specified. All reactions were monitored by thin layer chromatography (TLC) under 254 nm and 365 nm. TLC and column chromatography were performed on HG/T2354-92 GF254 thin layer chromatography silica gel plate and silica gel (200-300 mesh) respectively, both of which are produced by Qingdao Ocean Chemical Co., Ltd.. Melting points of the synthesized compounds were measured by RY-1 melting point meter of Tianjin Analytical instrument Factory. Mass spectrometry was recorded by Shimadzu LCMS-2020 mass spectrometer. ^{1}H NMR and ^{13}C NMR spectra were determined by Bruker AV-300 or Bruker Avance NEO 400 NMR spectrometer with TMS (tetramethylsilane) as the internal standard.

4.1.1 2-bromo-1-(2,4-difluorophenoxy)-4-nitrobenzene (**12**)

A solution of compound **11** (0.3 g, 1.36 mmol), 2,4-difluorophenol (0.266 g, 2.05 mmol) and potassium carbonate(0.376 g, 2.73 mmol) in DMF (3 mL) was stirred at 85°C for 3 h. After cooling to the room temperature, the reaction mixture was diluted with water and the precipitate was filtered. The filter cake was washed with water and dried to afford **12** (0.38 g, 84%) as a light yellow solid without further purification. ^{1}H NMR (300 MHz, $CDCl_3$) δ (ppm): 8.55 (d, J = 2.7 Hz, 1H), 8.10 (dd, J = 9.1, 2.7 Hz, 1H), 7.21 (td, J = 8.9, 5.5 Hz, 1H), 7.07-6.94 (m, 2H), 6.73 (d, J = 9.1 Hz, 1H).

4.1.2 3-bromo-4-(2,4-difluorophenoxy)aniline (**13**)

Iron powder (0.193 g, 3.45 mmol) was added in portions to a stirred solution of **12** (0.38 g, 1.15 mmol) in ethanol/THF/saturated ammonium chloride solution (15 mL, 1/1/1) at room temperature. The mixture was heated at 100°C for 2 h. After cooling to the room temperature, the reaction mixture was filtered through a celite pad and the filtrate was concentrated in vacuo. The residue was diluted with water and extracted with EtOAc. The combined organic layers were washed with brine, dried over Na_2SO_4, and concentrated to give compound **13** (0.312 g, 90%) as a brown solid without further purification. ^{1}H NMR (300 MHz, DMSO-d_6) δ (ppm): 7.40 (ddd, J = 11.7, 7.3, 3.0 Hz, 1H), 7.03-6.94 (m, 1H), 6.92-6.83 (m, 2H), 6.76 (td, J = 9.4, 5.5 Hz, 1H), 6.58 (dd, J = 8.7, 2.6 Hz, 1H), 5.33 (s, 2H).

4.1.3 N-(3-bromo-4-(2,4-difluorophenoxy)phenyl)ethanesulfonamide (**14**)

To a mixture of compound **13** (1.30 g, 4.33 mmol) and triethylamine (2.41 mL, 17.33 mmol) in DCM (5 mL) cooled to 0°C was added ethanesulfonyl chloride (1.23 mL, 13.00 mmol) in DCM dropwise and then stirred at room temperature for 3 h. The reaction mixture was evaporated in vacuo, diluted with water, and extracted with EtOAc. The combined organic layers were washed with brine, dried over Na_2SO_4, and concentrated in vacuo. The resulting intermediate was used without further purification and suspended in 1,4-dioxane/10% NaOH (10 mL, 1/1), then the mixture was heated at 100°C for 2 h. The reaction mixture was evaporated in vacuo, diluted with water, and extracted with EtOAc. The combined organic layers were washed with brine, dried over Na_2SO_4 and concentrated. The residue was purified by column chromatography on silica gel (EtOAc/petroleum ether, 1/10) to obtain the title compound **14** (1.45 g, 84%) as a light yellow solid. ^{1}H NMR (300 MHz, $CDCl_3$) δ (ppm): 7.52 (d, J = 2.6 Hz, 1H), 7.13 (dd, J = 8.8, 2.7 Hz, 1H), 7.06-6.93 (m, 2H), 6.91-6.82 (m, 1H), 6.75 (d, J = 8.8 Hz, 1H), 6.65 (s, 1H), 3.14 (q, J = 7.4 Hz, 2H), 1.40 (t, J = 7.4 Hz, 3H).

4.1.4 ethyl (Z)-3-(5-bromo-2-methoxy-3-nitropyridin-4-yl)-2-hydroxyacrylate (**16**)

To a solution of compound **15** (3.90 g, 15.79 mmol) and diethyl oxalate (3.22 mL, 23.68 mmol) in ethanol/ether (32 mL, 1/1) was added potassium ethoxide (1.59g, 18.94mmol) and then refluxed for 30 min. The reaction mixture was concentrated in vacuo, diluted with water, and extracted with

EtOAc. The combined organic layers were washed with brine, dried over Na_2SO_4, and concentrated in vacuo. The residue was purified by column chromatography on silica gel (EtOAc/petroleum ether, 1/10) to give **16** (1.72 g, 31%) as a light yellow solid. ^{1}H NMR (300 MHz, DMSO-d_6) δ (ppm): 10.56 (s, 1H), 8.65 (d, *J* = 13.3 Hz, 1H), 6.22 (s, 1H), 4.48 (s, 1H), 4.34-4.22 (m, 2H), 3.98 (d, *J* = 7.1 Hz, 3H), 1.35-1.24 (m, 3H).

4.1.5 ethyl 4-bromo-7-methoxy-1H-pyrrolo[2,3-c]pyridine-2-carboxylate (**17**)

In a solution of compound **16** (1.72 g, 4.96 mmol) in ethanol/acetic acid (30 mL, 1/1/) was added iron powder (0.83 g, 14.87 mmol) in portions at room temperature. The mixture was heated at 100°C for 2 h. After cooling to the room temperature, the reaction mixture was diluted with EtOAc and filtered through a celite pad. The filtrate was evaporated in vacuo, diluted with water, and extracted with EtOAc. The combined organic layers were washed with brine, dried over Na_2SO_4, and concentrated in vacuo. The residue was purified by column chromatography on silica gel (EtOAc/petroleum ether, 1/8) to obtain **17** (1.38 g, 93%) as a white solid. ^{1}H NMR (300 MHz, DMSO-d_6) δ (ppm): 13.06 (s, 1H), 7.84 (d, *J* = 1.4 Hz, 1H), 7.01 (s, 1H), 4.34 (q, *J* = 7.2 Hz, 2H), 4.02 (d, *J* = 1.2 Hz, 3H), 1.34 (dd, *J* = 7.8, 6.4 Hz, 3H).

4.1.6 ethyl 1-benzyl-4-bromo-7-methoxy-1H-pyrrolo[2,3-c]pyridine-2-carboxylate (**18**)

Benzyl bromide (0.822 mL, 6.92 mmol) was added to a stirred solution of compound **17** (1.38 g, 4.61 mmol) and potassium carbonate (1.28 g, 9.23 mmol) in DMF (10 mL) at room temperature. The solution was then heated to 80°C for 5 h. After cooling to the room temperature, the reaction solution was poured into ice water. The precipitated product was filtered, washed with water, and dried to afford the title compound **18** (1.75 g, 97%) as a light yellow solid without further purification. ^{1}H NMR (300 MHz, DMSO-d_6) δ (ppm): 7.90 (s, 1H), 7.31-7.18 (m, 4H), 6.95 (d, *J* = 6.9 Hz, 2H), 6.06 (s, 2H), 4.30 (q, *J* = 7.0 Hz, 2H), 3.94 (s, 3H), 1.28 (t, *J* = 7.1 Hz, 3H).

4.1.7 ethyl 1-benzyl-4-bromo-7-oxo-6,7-dihydro-1H-pyrrolo[2,3-c]pyridine-2-carboxylate (**19**)

A solution of compound **18** (1.75 g, 4.50 mmol) in 1,4-dioxane/4 N HCl (20 mL, 1/1) was stirred at 80°C for 2h. After cooling to the room temperature, the mixture was filtered. The filter cake was washed with water and dried to give the crude compound **19** (1.65 g, 98%) as a light yellow solid without further purification. ^{1}H NMR (300 MHz, DMSO-d_6) δ (ppm): 11.57 (s, 1H), 7.31-7.17 (m, 4H), 6.98 (s, 3H), 6.24 (s, 2H), 4.24 (q, *J* = 6.7 Hz, 2H), 1.24 (t, *J* = 6.5 Hz, 3H).

4.1.8 ethyl 1-benzyl-4-bromo-6-methyl-7-oxo-6,7-dihydro-1H-pyrrolo[2,3-c]pyridine-2-carboxylate (**20**)

In a solution of compound **19** (1.65 g, 4.40 mmol) and potassium carbonate (1.22 g, 8.79 mmol) in acetonitrile (30 mL) was added dimethyl sulfate (0.625 mL, 6.60 mmol) and then stirred at 70°C for 4 h. After cooling to the room temperature, the reaction mixture was filtered through a celite pad and washed with DCM. The filtrate was concentrated in vacuo and purified by column chromatography on silica gel (EtOAc/petroleum ether, 1/8) to afford compound **20** (1.47 g, 86%) as a white solid. ^{1}H NMR (300 MHz, DMSO-d_6) δ (ppm): 7.71 (s, 1H), 7.23 (dt, *J* = 13.4, 6.9 Hz, 3H), 6.96 (d, *J* = 6.5 Hz, 3H), 6.26 (s, 2H), 4.24 (q, *J* = 7.1 Hz, 2H), 3.47 (s, 3H), 1.24 (t, *J* = 7.1 Hz, 3H).

4.1.9 ethyl 1-benzyl-6-methyl-7-oxo-4-(4,4,5,5-tetramethyl-1,3,2-dioxaborolan-2-yl)-6,7-dihydro-1H-pyrrolo[2,3-c]pyridine-2-carboxylate (**21**)

A mixture of compound **20** (1.47 g, 3.76 mmol), bis(pinacolato)diboron (1.91 g, 7.53 mmol), tris(dibenzylideneacetone)dipalladium (0.172 g, 0.188 mmol), X-PHOS (0.179 g, 0.376 mmol) and potassium acetate (0.812 g, 0.828 mmol) in 1,4-dioxane (30 mL) was refluxed under nitrogen

atmosphere for 12 h. After cooling to the room temperature, the reaction mixture was diluted with EtOAc and water, and filtered through a celite. The aqueous layer was extracted with EtOAc. The combined organic layer of the filtrate was washed with water and brine, dried over Na_2SO_4, and concentrated in vacuo. The resultant was purified by column chromatography on silica gel (EtOAc/petroleum ether, 1/6) to obtain **21** (0.696 g, 42%) as a white solid. ^{1}H NMR (300 MHz, DMSO-d_6) δ (ppm): 7.65 (s, 1H), 7.29-7.14 (m, 4H), 6.92 (d, *J* = 7.0 Hz, 2H), 6.26 (s, 2H), 4.25 (q, *J* = 7.0 Hz, 2H), 3.52 (s, 3H), 1.31 (s, 12H), 1.23 (t, *J* = 7.1 Hz, 3H).

4.1.10 ethyl 1-benzyl-4-(2-(2,4-difluorophenoxy)-5-(ethylsulfonamido)phenyl)-6-methyl-7-oxo-6,7-dihydro-1H-pyrrolo[2,3-c]pyridine-2-carboxylate (**22**)

A solution of **21** (0.695 g, 1.59 mmol), **14** (0.521g，1.33mmol) , Pd(dppf)Cl_2·CH_2Cl_2 (0.054 g, 0.066 mmol) and potassium carbonate (0.367 g, 2.65 mmol) in toluene/MeOH/DMF (14 mL, 9/3/2) was heated to 80°C and stirred under nitrogen atmosphere for 12 h. After cooling to the room temperature, the reaction mixture was diluted with EtOAc and water, and filtered through a celite pad. The aqueous layer was extracted with EtOAc. The combined organic layers were washed with brine, dried over Na_2SO_4, and evaporated in vacuo. The residue was purified by column chromatography on silica gel (EtOAc/petroleum ether, 1/3) to give the title compound **22** (0.537 g, 65%) as a white solid. ^{1}H NMR (300 MHz, DMSO-d_6) δ (ppm): 9.83 (s, 1H), 7.44 (s, 1H), 7.35 (d, *J* = 2.6 Hz, 2H), 7.30-7.19 (m, 4H), 7.08-6.94 (m, 6H), 6.28 (s, 2H), 4.20 (q, *J* = 7.1 Hz, 2H), 3.52 (s, 3H), 3.13 (q, *J* = 7.4 Hz, 2H), 1.23 (q, *J* = 7.2 Hz, 6H).

4.1.11 ethyl 4-(2-(2,4-difluorophenoxy)-5-(ethylsulfonamido)phenyl)-6-methyl-7-oxo-6,7-dihydro-1H-pyrrolo[2,3-c]pyridine-2-carboxylate (**23**)

Compound **22** (0.537 g, 0.863 mmol) was dissolved in trifluoroacetic acid (3mL). Anisole (0.188 mL, 1.73 mmol) and concentrated sulfuric acid (0.23 mL, 4.32 mmol) were then added. The solution was stirred at 60°C for 6 h. After cooling to the room temperature, the reaction mixture was poured into ice water, quenched with saturated sodium bicarbonate solution and extracted with EtOAc. The combined organic layers were washed with brine, dried over Na_2SO_4 and concentrated in vacuo. The resultant was purified by column chromatography on silica gel (MeOH/DCM, 1/120) to give compound **23** (0.225 g, 49%) as a white solid. ^{1}H NMR (300 MHz, DMSO-d_6) δ (ppm): 12.90 (s, 1H), 9.82 (s, 1H), 7.36 (dd, *J* = 8.4, 4.5 Hz, 3H), 7.23 (dd, *J* = 8.8, 2.7 Hz, 1H), 7.08-6.93 (m, 3H), 6.84 (s, 1H), 4.26 (q, *J* = 7.1 Hz, 2H), 3.54 (s, 3H), 3.12 (q, *J* = 7.3 Hz, 2H), 1.26 (dt, *J* = 17.7, 7.2 Hz, 6H).

4.1.12 4-(2-(2,4-difluorophenoxy)-5-(ethylsulfonamido)phenyl)-6-methyl-7-oxo-6,7-dihydro-1H-pyrrolo[2,3-c] pyridine-2-carboxylic acid (**24**)

A solution of compound **23** (0.128 g, 0.241 mmol)) and lithium hydroxide (0.030 g, 0.722 mmol) in MeOH/H2O (3 mL, 2/1) was heated at 60°C for 2 h. After cooling to the room temperature, the reaction mixture was concentrated in vacuo, diluted with water and acidified with 1N HCl. The precipitated product was filtered, washed with water, and dried to give the crude compound **24** (0.115 g, 95%) as a white solid without further purification. ^{1}H NMR (400 MHz, DMSO-d_6) δ (ppm): 13.01 (s, 1H), 12.67 (s, 1H), 9.84 (s, 1H), 7.37 (dd, *J* = 14.4, 4.1 Hz, 3H), 7.23 (dd, *J* = 8.6, 2.7 Hz, 1H), 7.09-6.91 (m, 3H), 6.88-6.77 (m, 1H), 3.54 (s, 3H), 3.19-3.06 (m, 2H), 1.23 (t, *J* = 6.5 Hz, 3H).

4.1.13 4-(2-(2,4-difluorophenoxy)-5-(ethylsulfonamido)phenyl)-6-methyl-7-oxo-N-(prop-2-yn-1-yl)-6,7-dihydro-1H-pyrrolo[2,3-c]pyridine-2-carboxamide (**25**)

A mixture of compound **24** (1.60 g, 3.18 mmol), EDCI (0.731 g, 3.81 mmol), HOBT (0.515 g, 3.81 mmol) and triethylamine (0.883 mL, 6.6 mmol) in DMF was stirred at room temperature for

30 min and then added propargylamine (0.262 mL, 3.81 mmol). The reaction mixture was stirred at room temperature for 2h and then diluted with saturated ammonium chloride solution. The precipitated product was filtered, washed with water, and dried to give the crude compound **25** (1.47 g, 86%) as a off-white solid without further purification. ^{1}H NMR (300 MHz, DMSO-d_6) δ (ppm): 12.38 (s, 1H), 9.83 (s, 1H), 8.80 (s, 1H), 7.34 (d, *J* = 7.0 Hz, 3H), 7.24 (d, *J* = 8.6 Hz, 1H), 6.98 (dd, *J* = 18.4, 9.3 Hz, 3H), 6.89 (s, 1H), 4.05 (s, 2H), 3.53 (s, 3H), 3.19 (s, 1H), 3.11 (d, *J* = 7.0 Hz, 2H), 1.23 (s, 3H).

4.1.14 Synthetic procedures of the target compound **32a**

The target compound **32a** was synthesized from **26a** according to the following procedures, which can also be applied to the synthesis of the target compounds **32b-32d**.

4.1.14.1 2-hydroxyethyl 4-methylbenzenesulfonate (**27a**)

To a solution of compound **26a** (3.91 g, 62.95 mmol) in pyridine (5mL) was added paratoluensulfonyl chloride (6 g, 31.47 mmol) in portions and then stirred at room temperature for 4h. The reaction mixture was acidified with 6N HCl and extracted with EtOAc. The combined organic layers were washed with brine, dried over Na_2SO_4, and concentrated in vacuo. The residue was purified by column chromatography on silica gel (EtOAc/petroleum ether, 1/10) to afford **27a** (2 g, 29%) as a colorless liquid. ^{1}H NMR (300 MHz, $CDCl_3$) δ (ppm): 7.81 (d, *J* = 8.3 Hz, 2H), 7.36 (d, *J* = 8.0 Hz, 2H), 4.16-4.12 (m, 2H), 3.85 –3.78 (m, 2H), 2.45 (s, 3H), 2.01 (d, *J* = 19.0 Hz, 1H).

4.1.14.2 2-azidoethan-1-ol (**28a**)

A solution of compound **27a** (1.2 g, 5.55 mmol) and sodium azide (0.72 g, 11.1 mmol) of propanone/H_2O (10 mL, 1/1) was heated to reflux for 16h. The reaction mixture was diluted with water and extracted with EtOAc. The combined organic layers were washed with saturated sodium carbonate solution and brine, dried over Na_2SO_4, and evaporated in vacuo. The residue was purified by column chromatography on silica gel (EtOAc/petroleum ether, 1/30) to afford **28a** (0.41 g, 85%) as a colorless liquid. ^{1}H NMR (300 MHz, $CDCl_3$) δ (ppm): 3.82-3.74 (m, 2H), 3.49-3.39 (m, 2H), 2.01 (s, 1H).

4.1.14.3 tert-butyl 2-(2-azidoethoxy)acetate (**29a**)

To a solution of compound **28a** (0.41 g, 4.71 mmol) and tert-butyl bromoacetate (1.1 g, 5.65 mmol) in THF (15 mL) cooled to 0°C was added sodium hydride (0.38 g, 9.42 mmol) in small portions and kept at 0°C for 30 min. The slurry was then stirred at room temperature for 3h. The reaction mixture was quenched with methanol, diluted with water and extracted with EtOAc. The combined organic layers were washed with brine, dried over Na_2SO_4, and concentrated in vacuo. The residue was purified by column chromatography on silica gel (EtOAc/petroleum ether, 1/20) to obtain **29a** (0.41 g, 43%) as a colorless liquid. ^{1}H NMR (300 MHz, $CDCl_3$) δ (ppm): 4.06-4.00 (m, 2H), 3.76-3.70 (m, 2H), 3.48-3.41 (m, 2H), 1.49 (d, *J* = 5.8 Hz, 9H).

4.1.14.4 2-(2-azidoethoxy)acetic acid (**30a**)

In a solution of compound **29a** (0.41 g，2.04 mmol) in DCM (4 mL) was added trifluoroacetic acid (1 mL) and then stirred at room temperature for 3h. The reaction mixture was concentrated in vacuo to give **30a** (0.29 g, 98%) as a brown liquid without further purification.

4.1.14.5 2-(2-azidoethoxy)-N-(2-(2,6-dioxopiperidin-3-yl)-1-oxoisoindolin-4-yl)acetamide (**31a**)

To a solution of **30a** (0.29 g, 2.03 mmol) in DCM were added thionyl chloride (1 mL) and two drops of DMF at room temperature. The mixture was then refluxed for 4h. The reaction mixture was evaporated in vacuo and the resulting acyl chloride was used without further purification. To a solution of lenalidomide (0.3 g, 1.16 mmol) in 1-methyl-2-pyrrolidinone (3 ml) was added the acyl

chloride and then stirred at room temperature for 4 h. The reaction mixture was diluted with water and extracted with EtOAc. The combined organic layers were washed with brine, dried over Na_2SO_4, and concentrated in vacuo. The residue was purified by column chromatography on silica gel (MeOH/DCM, 1/100) to afford **31a** (0.26 g, 58%) as a yellow solid. ^{1}H NMR (400 MHz, DMSO-d_6) δ (ppm): 11.02 (s, 1H), 9.74 (s, 1H), 7.77 (d, *J* = 7.4 Hz, 1H), 7.54 (dt, *J* = 15.3, 7.5 Hz, 2H), 5.23-5.10 (m, 1H), 4.37 (q, *J* = 17.3 Hz, 2H), 4.18 (s, 2H), 3.75 (d, *J* = 4.4 Hz, 2H), 3.52 (d, *J* = 4.3 Hz, 2H), 3.02-2.85 (m, 1H), 2.60 (d, *J* = 17.9 Hz, 1H), 2.35 (d, *J* = 12.8 Hz, 1H), 2.03 (s, 1H).

4.1.14.6 4-(2-(2,4-difluorophenoxy)-5-(ethylsulfonamido)phenyl)-N-((1-(2-(2-((2-(2,6-dioxopiperidin-3-yl)-1-oxoisoindolin-4-yl)amino)-2-oxoethoxy)ethyl)-1H-1,2,3-triazol-4-yl)methyl)-6-methyl-7-oxo-6,7-dihydro-1H-pyrrolo[2,3-c]pyridine-2-carboxamide (**32a**)

A solution of compound **25** (0.06 g, 0.111 mmol), **31a** (0.06 g, 0.111 mmol) and copper sulfate pentahydrate (0.009 g, 0.044 mmol) in DCM/MeOH/H_2O was stirred at room temperature for 10 min, and sodium ascorbate (0.006 g, 0.022 mmol) was added. Then the mixture was stirred at room temperature for 4h. The reaction mixture was diluted with water and extracted with DCM. The combined organic layers were washed with brine, dried over Na_2SO_4, and evaporated in vacuo. The residue was purified by column chromatography on silica gel (MeOH/DCM, 1/30) to give the target compound **32a** (0.069 g, 59%) as a light yellow solid. m.p.: 186-190 °C; ^{1}H NMR (400 MHz, DMSO-d_6) δ (ppm) : 12.34 (s, 1H), 11.01 (s, 1H), 9.76 (d, *J* = 51.5 Hz, 2H), 8.88 (s, 1H), 8.07 (s, 1H), 7.74 (s, 1H), 7.51 (d, *J* = 20.4 Hz, 2H), 7.28 (d, *J* = 48.0 Hz, 4H), 6.97 (dd, *J* = 40.7, 23.7 Hz, 4H), 5.14 (s, 1H), 4.61 (s, 2H), 4.50 (s, 2H), 4.38 (d, *J* = 12.0 Hz, 2H), 4.14 (s, 2H), 3.96 (s, 2H), 3.53 (s, 3H), 3.10 (s, 2H), 2.91 (s, 1H), 2.58 (s, 1H), 2.42-2.32 (m, 1H), 2.02 (s, 1H), 1.22 (s, 3H); ^{13}C NMR (101 MHz, DMSO-d_6) δ (ppm): 173.38, 171.49, 168.54, 168.27, 159.96, 154.63, 150.76, 144.86, 140.23, 135.15, 134.63, 133.63, 133.21, 130.52, 129.59, 129.26, 127.93, 126.68, 124.83, 124.10, 123.65, 122.15, 121.35, 120.21, 118.69, 112.27, 110.54, 106.05, 105.71, 69.91, 69.61, 52.02, 49.76, 46.91, 45.58, 36.29, 34.89, 31.65, 23.01, 8.49; MS (ESI) m/z: calculated for $C_{43}H_{40}F_2N_{10}O_{10}S$ $[M-H]^-$: 925.26, found: 925.00.

4.1.15 4-(2-(2,4-difluorophenoxy)-5-(ethylsulfonamido)phenyl)-N-((1-(2-(2-(2-((2-(2,6-dioxopiperidin-3-yl)-1-oxoisoindolin-4-yl)amino)-2-oxoethoxy)ethoxy)ethyl)-1H-1,2,3-triazol-4-yl)methyl)-6-methyl-7-oxo-6,7-dihydro-1H-pyrrolo[2,3-c]pyridine-2-carboxamide (**32b)**

Compound **32b** (0.138g, 66%) as a light yellow solid. m.p.: 176-180 °C; ^{1}H NMR (400 MHz, DMSO-d_6) δ (ppm) : 12.35 (s, 1H), 11.01 (s, 1H), 9.83 (s, 1H), 9.68 (s, 1H), 8.87 (s, 1H), 7.99 (s, 1H), 7.72 (d, *J* = 7.9 Hz, 1H), 7.54 (d, *J* = 7.0 Hz, 1H), 7.52-7.45 (m, 1H), 7.34 (d, *J* = 6.6 Hz, 3H), 7.22 (d, *J* = 8.7 Hz, 1H), 7.06 (d, *J* = 6.0 Hz, 1H), 7.00 (d, *J* = 7.8 Hz, 1H), 6.95-6.81 (m, 2H), 5.13 (d, *J* = 8.5 Hz, 1H), 4.50 (d, *J* = 12.7 Hz, 4H), 4.43-4.30 (m, 2H), 4.09 (s, 2H), 3.84 (s, 2H), 3.62 (d, *J* = 4.5 Hz, 4H), 3.52 (s, 3H), 3.10 (d, *J* = 7.1 Hz, 2H), 2.89 (d, *J* = 12.6 Hz, 1H), 2.60 (s, 1H), 2.35 (d, *J* = 13.8 Hz, 1H), 2.00 (d, *J* = 10.0 Hz, 1H), 1.24-1.20 (t, 3H); ^{13}C NMR (101 MHz, DMSO-d_6) δ (ppm): 173.34, 171.51, 168.83, 168.25, 159.93, 154.62, 150.75, 144.77, 140.30, 135.25, 134.65, 133.64, 133.27, 130.53, 129.36, 129.09, 127.96, 126.77, 124.86, 123.93, 123.62, 122.30, 121.28, 120.16, 118.70, 112.26, 110.48, 106.32, 105.72, 70.66, 70.39, 69.84, 69.23, 52.01, 49.75, 46.90, 45.56, 36.27, 34.88, 31.66, 23.03, 8.51; MS (ESI) m/z: calculated for $C_{45}H_{44}F_2N_{10}O_{11}S$ $[M-H]^-$: 969.29, found: 969.06.

4.1.15 4-(2-(2,4-difluorophenoxy)-5-(ethylsulfonamido)phenyl)-N-((1-(2-(2-(2-(2-((2-(2,6-dioxopiperidin-3-yl)-1-oxoisoindolin-4-yl)amino)-2-oxoethoxy)ethoxy)ethoxy)ethyl)-1H-1,2,3-

triazol-4-yl)methyl)-6-methyl-7-oxo-6,7-dihydro-1H-pyrrolo[2,3-c]pyridine-2-carboxamide (**32c)** Compound **32c** (0.085 g, 70%) as a yellow solid. m.p.: 144-148 °C; ^{1}H NMR (300 MHz, DMSO-d_6) δ (ppm) : 12.33 (s, 1H), 11.00 (s, 1H), 9.82 (s, 1H), 9.67 (s, 1H), 8.86 (s, 1H), 7.96 (s, 1H), 7.73 (d, *J* = 7.5 Hz, 1H), 7.52 (dt, *J* = 15.0, 7.5 Hz, 2H), 7.40-7.30 (m, 3H), 7.23 (dd, *J* = 8.8, 2.6 Hz, 1H), 7.13-6.97 (m, 2H), 6.94 (d, *J* = 8.7 Hz, 1H), 6.89 (d, *J* = 2.2 Hz, 1H), 5.14 (dd, *J* = 13.3, 5.0 Hz, 1H), 4.48 (dd, *J* = 9.3, 4.9 Hz, 4H), 4.37 (d, *J* = 6.7 Hz, 2H), 4.11 (s, 2H), 3.77 (t, *J* = 5.0 Hz, 2H), 3.64-3.61 (m, 2H), 3.54 (d, *J* = 4.7 Hz, 2H), 3.53 (s, 3H), 3.50 (s, 4H), 3.11 (d, *J* = 7.4 Hz, 2H), 2.96-2.86 (m, 1H), 2.59 (d, *J* = 17.7 Hz, 1H), 2.36 (d, *J* = 9.1 Hz, 1H), 2.02 (s, 1H), 1.22 (t, *J* = 5.6 Hz, 3H); ^{13}C NMR (126 MHz, DMSO-d_6) δ (ppm): 172.86, 170.98, 168.47, 167.83, 159.50, 154.20, 150.33, 144.30, 139.90, 134.84, 134.19, 133.18, 132.88, 132.72, 130.05, 128.97, 128.68, 127.51, 126.36, 124.37, 123.39, 123.24, 121.66, 120.94, 119.79, 118.28, 111.79, 110.12, 105.65, 70.38, 69.96, 69.62, 69.54, 68.72, 51.63, 49.32, 46.50, 45.23, 35.80, 34.42, 31.19, 22.56, 8.01; MS (ESI) m/z: calculated for $C_{47}H_{48}F_2N_{10}O_{12}S$ $[M-H]^-$: 1013.31, found: 1013.05.

4.1.15 4-(2-(2,4-difluorophenoxy)-5-(ethylsulfonamido)phenyl)-N-((1-(14-((2-(2,6-dioxopiperidin-3-yl)-1-oxoisoindolin-4-yl)amino)-14-oxo-3,6,9,12-tetraoxatetradecyl)-1H-1,2,3-triazol-4-yl)methyl)-6-methyl-7-oxo-6,7-dihydro-1H-pyrrolo[2,3-c]pyridine-2-carboxamide (**32d)**

Compound **32d** (0.091 g, 84%) as a light yellow solid. m.p.: 130-134 °C; ^{1}H NMR (300 MHz, DMSO-d_6) δ (ppm) : 12.34 (s, 1H), 11.00 (s, 1H), 9.82 (s, 1H), 9.67 (s, 1H), 8.86 (s, 1H), 7.95 (s, 1H), 7.72 (d, *J* = 7.2 Hz, 1H), 7.52 (dt, *J* = 15.1, 7.4 Hz, 2H), 7.34 (s, 3H), 7.23 (d, *J* = 8.9 Hz, 1H), 7.03 (dd, *J* = 17.9, 8.3 Hz, 2H), 6.96-6.87 (m, 2H), 5.14 (d, *J* = 8.6 Hz, 1H), 4.48 (s, 4H), 4.37 (d, *J* = 6.4 Hz, 2H), 4.12 (s, 2H), 3.77 (s, 2H), 3.65 (s, 2H), 3.54 (s, 2H), 3.53 (s, 3H), 3.43 (d, *J* = 11.6 Hz, 8H), 3.10 (d, *J* = 7.4 Hz, 2H), 2.91 (t, *J* = 12.9 Hz, 1H), 2.59 (d, *J* = 17.7 Hz, 1H), 2.34 (t, *J* = 13.6 Hz, 1H), 1.99 (d, *J* = 4.4 Hz, 1H), 1.23-1.21 (t, 3H); ^{13}C NMR (101 MHz, DMSO-d_6) δ (ppm): 173.35, 171.50, 168.93, 168.27, 167.40, 159.93, 154.65, 150.76, 144.75, 140.33 (d, J = 11.7 Hz), 135.35, 134.66, 133.66, 133.28, 131.95, 130.52, 129.39, 129.12, 127.96, 126.84, 124.86, 123.86, 123.64, 122.13, 121.31, 120.24, 118.68, 112.38, 112.15, 110.53, 106.11, 70.84, 70.59, 69.18, 61.80, 52.03, 49.79, 46.93, 45.59, 36.28, 34.89, 31.67, 23.04, 8.50; MS (ESI) m/z: calculated for $C_{49}H_{52}F_2N_{10}O_{13}S$ $[M+Na]^+$: 1081.34, found: 1081.20.

4.2. Biological evaluation

4.2.1 BRD4 BD1 binding affinity assay

The binding affinity assay was administered by Shanghai ChemPartner Co. Firstly 1× assay buffer was prepared using modified HEPES Buffer. Compounds were transferred to assay plate by Echo and DMSO's final concentration is 0.1%. The preparation of protein solution and substrate solution was performed in 1x assay buffer. After that, 5 μL of protein solution or 5 μL of 1x assay buffer was transferred to assay plate with an incubation at room temperature for 15 min. Then 5 μL of substrate solution was added to each well to start reaction, followed by an incubation at room temperature for 60 min. Next, 15 μL acceptor and donor solution were added and incubated at room temperature for 60 min under subdued light. Finally, the IC_{50} values were calculated from datas readed by EnSpire with Alpha mode.

4.2.2 Cell culture

BxPC3 cell line from Key laboratory of SATCM for Empirical Formulae Evaluation and Achievements Transformation was cultured in the Dulbecco's Modified Eagle Medium (DMEM) medium (YUANPEI, CHINA) supplemented with 10% fetal bovine serum (FBS) (BI, USA) and routinely maintained at 37℃， 5% CO2 incubator.

4.2.3 Cell proliferation assay

The cell proliferation assay was evaluated by MTT assay. BxPC3 cells ($4x10^3$ cells) were seeded in 96-well plates with 100 μL of culture medium and incubated at 37℃ and an atmosphere of 5% CO_2 for 24 h. The cells were then treated with medium containing various concentrations of compounds and 1‰ DMSO, with every concentration was repeated in four wells. 1‰ DMSO solution was set to the control group. After that, cells were further incubated for 72 h. Then each well of the cells was added 20 μL of MTT reagent and incubated for 3 h at 37℃ in standard culture conditions. The absorbance was measured in a microplate reader at 490 nm. The data were normalized to the DMSO control. The IC_{50} was calculated by GraphPad Prism 5 statistical software.

4.2.4 Western blotting analysis

BxPC3 cells were lysed with RIPA lysis buffer containing 1% PMSF and protease and phosphatase inhibitors. The protein concentration was determined with a BCA assay kit. Equal amounts of protein for each sample were separated using SDS-PAGE gels and transferred onto PVDF membranes. The membranes were subsequently blocked in 5% BSA for 1h at room temperature, followed by incubation with primary antibody overnight at 4℃. The membranes were then washed with 1X PBST and incubated with a secondary antibody for 1h. Finally, the membranes were treated with ECL detection reagents and exposed in the chemiluminescent imaging system.

4.2.5 Cell cycle progression analysis

BxPC3 cells were incubated in the absence or presence of compounds for 48h. Then cells were collected and fixed by 70% alcohol for 8 h at -20℃. The percentage of cells cycles was analyzed by staining with PI for 20 min at room temperature, followed by flow cytometry.

4.2.6 Cell apoptosis analysis

For the cell apoptosis assay, BxPC3 cells were incubated in the absence or presence of compounds for 48h. The percentage of apoptotic cells was analyzed by staining with fluorescein isothiocyanate-conjugated Annexin V and propidium iodide for 20 min at room temperature, followed by flow cytometry.

4.2.7 Live-dead staining

BxPC3 cells were seeded at $4x10^4$ cells/well in 12-well plates. After 48 h of compounds treatment, each well of the cells was stained with Live-Dead dye and incubated for 30 min at 37℃ in standard culture conditions. The fluorescence was photographed by an Inverted fluorescence Microscope.

Acknowledgments

This study was supported by the Natural Science Foundation of Jiangsu Province (No. BK 20141349) and the China National Key HiTech Innovation Project for the R&D of Novel Drugs (No.2013ZX09301303-002).

References

[1] A. Galvani, C. Thiriet. Nucleosome Dancing at the Tempo of Histone Tail Acetylation, Genes (Basel). 6 (2015) 607-621.

[2] P. Filippakopoulos, S. Knapp. Targeting bromodomains: epigenetic readers of lysine acetylation, Nat Rev Drug Discov. 13 (2014) 337-356.

[3] C.-w. Chung, D.F. Tough. Bromodomains: a new target class for small molecule drug discovery, Drug Discovery Today: Therapeutic Strategies. 9

(2012) e111-e120.

[4] C.H. Arrowsmith, C. Bountra, P.V. Fish, K. Lee, M. Schapira. Epigenetic protein families: a new frontier for drug discovery, Nat Rev Drug Discov. 11 (2012) 384-400.

[5] M.K. Jang, K. Mochizuki, M. Zhou, H.S. Jeong, J.N. Brady, K. Ozato. The bromodomain protein Brd4 is a positive regulatory component of P-TEFb and stimulates RNA polymerase II-dependent transcription, Mol Cell. 19 (2005) 523-534.

[6] F. Wang, H. Liu, W.P. Blanton, A. Belkina, N.K. Lebrasseur, G.V. Denis. Brd2 disruption in mice causes severe obesity without Type 2 diabetes, Biochem J. 425 (2009) 71-83.

[7] J.M. Lamonica, W. Deng, S. Kadauke, A.E. Campbell, R. Gamsjaeger, H. Wang, Y. Cheng, A.N. Billin, R.C. Hardison, J.P. Mackay, G.A. Blobel. Bromodomain protein Brd3 associates with acetylated GATA1 to promote its chromatin occupancy at erythroid target genes, Proc Natl Acad Sci U S A. 108 (2011) E159-168.

[8] J. Gaucher, F. Boussouar, E. Montellier, S. Curtet, T. Buchou, S. Bertrand, P. Hery, S. Jounier, A. Depaux, A.L. Vitte, P. Guardiola, K. Pernet, A. Debernardi, F. Lopez, H. Holota, J. Imbert, D.J. Wolgemuth, M. Gerard, S. Rousseaux, S. Khochbin. Bromodomain-dependent stage-specific male genome programming by Brdt, EMBO J. 31 (2012) 3809-3820.

[9] Z. Yang, J.H. Yik, R. Chen, N. He, M.K. Jang, K. Ozato, Q. Zhou. Recruitment of P-TEFb for stimulation of transcriptional elongation by the bromodomain protein Brd4, Mol Cell. 19 (2005) 535-545.

[10] S. Schroder, S. Cho, L. Zeng, Q. Zhang, K. Kaehlcke, L. Mak, J. Lau, D. Bisgrove, M. Schnolzer, E. Verdin, M.M. Zhou, M. Ott. Two-pronged binding with bromodomain-containing protein 4 liberates positive transcription elongation factor b from inactive ribonucleoprotein complexes, J Biol Chem. 287 (2012) 1090-1099.

[11] C.V. Dang. MYC, microRNAs and glutamine addiction in cancers, Cell Cycle. 8 (2009) 3243-3245.

[12] J.A. Mertz, A.R. Conery, B.M. Bryant, P. Sandy, S. Balasubramanian, D.A. Mele, L. Bergeron, R.J. Sims, 3rd. Targeting MYC dependence in cancer by inhibiting BET bromodomains, Proc Natl Acad Sci U S A. 108 (2011) 16669-16674.

[13] M.A. Dawson, R.K. Prinjha, A. Dittmann, G. Giotopoulos, M. Bantscheff, W.I. Chan, S.C. Robson, C.W. Chung, C. Hopf, M.M. Savitski, C. Huthmacher, E. Gudgin, D. Lugo, S. Beinke, T.D. Chapman, E.J. Roberts, P.E. Soden, K.R. Auger, O. Mirguet, K. Doehner, R. Delwel, A.K. Burnett, P. Jeffrey, G. Drewes, K. Lee, B.J. Huntly, T. Kouzarides. Inhibition of BET recruitment to chromatin as an effective treatment for MLL-fusion leukaemia, Nature. 478 (2011) 529-533.

[14] P. Filippakopoulos, J. Qi, S. Picaud, Y. Shen, W.B. Smith, O. Fedorov, E.M. Morse, T. Keates, T.T. Hickman, I. Felletar, M. Philpott, S. Munro, M.R.

McKeown, Y. Wang, A.L. Christie, N. West, M.J. Cameron, B. Schwartz, T.D. Heightman, N. La Thangue, C.A. French, O. Wiest, A.L. Kung, S. Knapp, J.E. Bradner. Selective inhibition of BET bromodomains, Nature. 468 (2010) 1067-1073.

[15] I.A. Asangani, V.L. Dommeti, X. Wang, R. Malik, M. Cieslik, R. Yang, J. Escara-Wilke, K. Wilder-Romans, S. Dhanireddy, C. Engelke, M.K. Iyer, X. Jing, Y.M. Wu, X. Cao, Z.S. Qin, S. Wang, F.Y. Feng, A.M. Chinnaiyan. Therapeutic targeting of BET bromodomain proteins in castration-resistant prostate cancer, Nature. 510 (2014) 278-282.

[16] P.K. Mazur, A. Herner, S.S. Mello, M. Wirth, S. Hausmann, F.J. Sanchez-Rivera, S.M. Lofgren, T. Kuschma, S.A. Hahn, D. Vangala, M. Trajkovic-Arsic, A. Gupta, I. Heid, P.B. Noel, R. Braren, M. Erkan, J. Kleeff, B. Sipos, L.C. Sayles, M. Heikenwalder, E. Hessmann, V. Ellenrieder, I. Esposito, T. Jacks, J.E. Bradner, P. Khatri, E.A. Sweet-Cordero, L.D. Attardi, R.M. Schmid, G. Schneider, J. Sage, J.T. Siveke. Combined inhibition of BET family proteins and histone deacetylases as a potential epigenetics-based therapy for pancreatic ductal adenocarcinoma, Nat Med. 21 (2015) 1163-1171.

[17] O. Mirguet, R. Gosmini, J. Toum, C.A. Clement, M. Barnathan, J.M. Brusq, J.E. Mordaunt, R.M. Grimes, M. Crowe, O. Pineau, M. Ajakane, A. Daugan, P. Jeffrey, L. Cutler, A.C. Haynes, N.N. Smithers, C.W. Chung, P. Bamborough, I.J. Uings, A. Lewis, J. Witherington, N. Parr, R.K. Prinjha, E. Nicodeme. Discovery of epigenetic regulator I-BET762: lead optimization to afford a clinical candidate inhibitor of the BET bromodomains, J Med Chem. 56 (2013) 7501-7515.

[18] C. Berthon, E. Raffoux, X. Thomas, N. Vey, C. Gomez-Roca, K. Yee, D.C. Taussig, K. Rezai, C. Roumier, P. Herait, C. Kahatt, B. Quesnel, M. Michallet, C. Recher, F. Lokiec, C. Preudhomme, H. Dombret. Bromodomain inhibitor OTX015 in patients with acute leukaemia: a dose-escalation, phase 1 study, The Lancet Haematology. 3 (2016) e186-e195.

[19] K.T. Siu, J. Ramachandran, A.J. Yee, H. Eda, L. Santo, C. Panaroni, J.A. Mertz, R.J. Sims Iii, M.R. Cooper, N. Raje. Preclinical activity of CPI-0610, a novel small-molecule bromodomain and extra-terminal protein inhibitor in the therapy of multiple myeloma, Leukemia. 31 (2017) 1760-1769.

[20] S.A. Piha-Paul, J.C. Sachdev, M. Barve, P. LoRusso, R. Szmulewitz, S.P. Patel, P.N. Lara, Jr., X. Chen, B. Hu, K.J. Freise, D. Modi, A. Sood, J.E. Hutti, J. Wolff, B.H. O'Neil. First-in-Human Study of Mivebresib (ABBV-075), an Oral Pan-Inhibitor of Bromodomain and Extra Terminal Proteins, in Patients with Relapsed/Refractory Solid Tumors, Clin Cancer Res. 25 (2019) 6309-6319.

[21] L.T. Lam, X. Lin, E.J. Faivre, Z. Yang, X. Huang, D.M. Wilcox, R.J. Bellin, S. Jin, S.K. Tahir, M. Mitten, T. Magoc, A. Bhathena, W.M. Kati, D.H. Albert, Y. Shen, T. Uziel. Vulnerability of Small-Cell Lung Cancer to Apoptosis Induced by the Combination of BET Bromodomain Proteins and BCL2 Inhibitors, Mol Cancer Ther. 16 (2017) 1511-1520.

[22] S. Shu, C.Y. Lin, H.H. He, R.M. Witwicki, D.P. Tabassum, J.M. Roberts, M.

Janiszewska, S.J. Huh, Y. Liang, J. Ryan, E. Doherty, H. Mohammed, H. Guo, D.G. Stover, M.B. Ekram, J. Brown, C. D'Santos, I.E. Krop, D. Dillon, M. McKeown, C. Ott, J. Qi, M. Ni, P.K. Rao, M. Duarte, S.Y. Wu, C.M. Chiang, L. Anders, R.A. Young, E. Winer, A. Letai, W.T. Barry, J.S. Carroll, H. Long, M. Brown, X.S. Liu, C.A. Meyer, J.E. Bradner, K. Polyak. Response and resistance to BET bromodomain inhibitors in triple-negative breast cancer, Nature. 529 (2016) 413-417.

[23] C.Y. Fong, O. Gilan, E.Y.N. Lam, A.F. Rubin, S. Ftouni, D. Tyler, K. Stanley, D. Sinha, P. Yeh, J. Morison. BET inhibitor resistance emerges from leukaemia stem cells, Nature.

[24] J. Lu, Y. Qian, M. Altieri, H. Dong, J. Wang, K. Raina, J. Hines, James D. Winkler, Andrew P. Crew, K. Coleman, Craig M. Crews. Hijacking the E3 Ubiquitin Ligase Cereblon to Efficiently Target BRD4, Chemistry & Biology. 22 (2015) 755-763.

[25] G.E. Winter, D.L. Buckley, J. Paulk, J.M. Roberts, A. Souza, S. Dhe-Paganon, J.E. Bradner. Phthalimide conjugation as a strategy for in vivo target protein degradation, Science. 348 (2015) 1376-1381.

[26] A.C. Lai, M. Toure, D. Hellerschmied, J. Salami, S. Jaime-Figueroa, E. Ko, J. Hines, C.M. Crews. Modular PROTAC Design for the Degradation of Oncogenic BCR-ABL, Angew Chem Int Ed Engl. 55 (2016) 807-810.

[27] S. Su, Z. Yang, H. Gao, H. Yang, S. Zhu, Z. An, J. Wang, Q. Li, S. Chandarlapaty, H. Deng, W. Wu, Y. Rao. Potent and Preferential Degradation of CDK6 via Proteolysis Targeting Chimera Degraders, J Med Chem. 62 (2019) 7575-7582.

[28] J. Yang, Y. Li, A. Aguilar, Z. Liu, C.Y. Yang, S. Wang. Simple Structural Modifications Converting a Bona fide MDM2 PROTAC Degrader into a Molecular Glue Molecule: A Cautionary Tale in the Design of PROTAC Degraders, J Med Chem. 62 (2019) 9471-9487.

[29] M. Zengerle, K.H. Chan, A. Ciulli. Selective Small Molecule Induced Degradation of the BET Bromodomain Protein BRD4, Acs Chemical Biology. 10 (2015) 1770-1777.

[30] T.K. Neklesa, J.D. Winkler, C.M. Crews. Targeted protein degradation by PROTACs, Pharmacol Ther. 174 (2017) 138-144.

[31] K. Raina, C.M. Crews. Targeted protein knockdown using small molecule degraders, Curr Opin Chem Biol. 39 (2017) 46-53.

[32] T. Ito, H. Ando, T. Suzuki, T. Ogura, K. Hotta, Y. Imamura, Y. Yamaguchi, H. Handa. Identification of a Primary Target of Thalidomide Teratogenicity, Science. 327 (2010) 1345-1350.

[33] E.S. Fischer, K. Bohm, J.R. Lydeard, H. Yang, M.B. Stadler, S. Cavadini, J. Nagel, F. Serluca, V. Acker, G.M. Lingaraju, R.B. Tichkule, M. Schebesta, W.C. Forrester, M. Schirle, U. Hassiepen, J. Ottl, M. Hild, R.E. Beckwith, J.W. Harper, J.L. Jenkins, N.H. Thoma. Structure of the DDB1-CRBN E3 ubiquitin ligase in complex with thalidomide, Nature. 512 (2014) 49-53.

[34] K. Raina, J. Lu, Y. Qian, M. Altieri, D. Gordon, A.M.K. Rossi, J. Wang, X.

Chen, H. Dong, K. Siu, J.D. Winkler, A.P. Crew, C.M. Crews, K.G. Coleman. PROTAC-induced BET protein degradation as a therapy for castration-resistant prostate cancer, Proceedings of the National Academy of Sciences. 113 (2016) 7124-7129.

[35] B. Zhou, J. Hu, F. Xu, Z. Chen, L. Bai, E. Fernandez-Salas, M. Lin, L. Liu, C.Y. Yang, Y. Zhao, D. McEachern, S. Przybranowski, B. Wen, D. Sun, S. Wang. Discovery of a Small-Molecule Degrader of Bromodomain and Extra-Terminal (BET) Proteins with Picomolar Cellular Potencies and Capable of Achieving Tumor Regression, J Med Chem. 61 (2018) 462-481.

[36] L. Bai, B. Zhou, C.Y. Yang, J. Ji, D. McEachern, S. Przybranowski, H. Jiang, J. Hu, F. Xu, Y. Zhao, L. Liu, E. Fernandez-Salas, J. Xu, Y. Dou, B. Wen, D. Sun, J. Meagher, J. Stuckey, D.F. Hayes, S. Li, M.J. Ellis, S. Wang. Targeted Degradation of BET Proteins in Triple-Negative Breast Cancer, Cancer Res. 77 (2017) 2476-2487.

[37] E.J. Faivre, D. Wilcox, X. Lin, P. Hessler, M. Torrent, W. He, T. Uziel, D.H. Albert, K. McDaniel, W. Kati, Y. Shen. Exploitation of Castration-Resistant Prostate Cancer Transcription Factor Dependencies by the Novel BET Inhibitor ABBV-075, Mol Cancer Res. 15 (2017) 35-44.

[38] K.F. McDaniel, L. Wang, T. Soltwedel, S.D. Fidanze, L.A. Hasvold, D. Liu, R.A. Mantei, J.K. Pratt, G.S. Sheppard, M.H. Bui, E.J. Faivre, X. Huang, L. Li, X. Lin, R. Wang, S.E. Warder, D. Wilcox, D.H. Albert, T.J. Magoc, G. Rajaraman, C.H. Park, C.W. Hutchins, J.J. Shen, R.P. Edalji, C.C. Sun, R. Martin, W. Gao, S. Wong, G. Fang, S.W. Elmore, Y. Shen, W.M. Kati. Discovery of N-(4-(2,4-Difluorophenoxy)-3-(6-methyl-7-oxo-6,7-dihydro-1H-pyrrolo[2,3-c]pyridin -4-yl)phenyl)ethanesulfonamide (ABBV-075/Mivebresib), a Potent and Orally Available Bromodomain and Extraterminal Domain (BET) Family Bromodomain Inhibitor, J Med Chem. 60 (2017) 8369-8384.

[39] M.H. Bui, X. Lin, D.H. Albert, L. Li, L.T. Lam, E.J. Faivre, S.E. Warder, X. Huang, D. Wilcox, C.K. Donawho, G.S. Sheppard, L. Wang, S. Fidanze, J.K. Pratt, D. Liu, L. Hasvold, T. Uziel, X. Lu, F. Kohlhapp, G. Fang, S.W. Elmore, S.H. Rosenberg, K.F. McDaniel, W.M. Kati, Y. Shen. Preclinical Characterization of BET Family Bromodomain Inhibitor ABBV-075 Suggests Combination Therapeutic Strategies, Cancer Res. 77 (2017) 2976-2989.

[40] L. Wang, Y. Dai, J. Holms, et al. Bromodomain inhibitors. WO 2014/206150 A1, December 31, 2014.

[41] L. Wang, J.K. Pratt, K.F. Mcdaniel, et al. Bromodomain inhibitors. WO 2013/097601 Al, July 4, 2013.

[42] A.P. Crew, K. Raina, H. Dong, Y. Qian, J. Wang, D. Vigil, Y.V. Serebrenik, B.D. Hamman, A. Morgan, C. Ferraro, K. Siu, T.K. Neklesa, J.D. Winkler, K.G. Coleman, C.M. Crews. Identification and Characterization of Von Hippel-Lindau-Recruiting Proteolysis Targeting Chimeras (PROTACs) of TANK-Binding Kinase 1, Journal of Medicinal Chemistry. 61 (2018) 583-598.

Authors have no conflict of interest to declare.

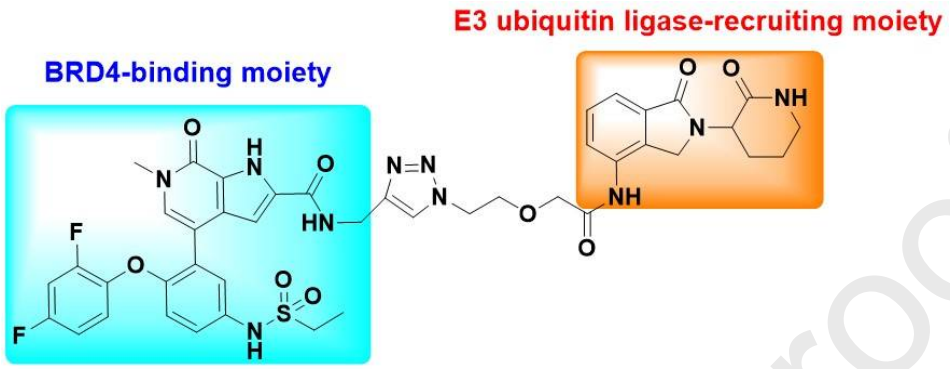

Induces potent degradation of BRD4 in BxPC3 cells
Shows significant anti-proliferative effect against BxPC3 cells (IC_{50} = 0.165 μM)

Several pyrrolopyrridone derivative-based BRD4 degraders were synthesized and evaluated in AlphaScreen assay and cell-based assays.

Degraders **32a** and **32b** effectively inhibited the proliferation of pancreatic cancer cell line BxPC3.

Degrader **32a** potently degraded BRD4 protein and inhibited the expression of c-Myc in a time-dependent manner.

Degrader **32a** induced the cell cycle arrest and apoptosis of BxPC3 cells.